Solid State Ionics 393 (2023) 116169

Contents lists available at ScienceDirect

Solid State Ionics

journal homepage: www.elsevier.com/locate/ssi

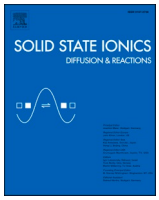

Accounting for stray capacitances in impedance measuring cells — A mandatory step in the investigation of solid ion conductors

Alexander Komar [a], Dirk Wilmer [b], H. Martin R. Wilkening [a,c], Ilie Hanzu [a,c,*]

[a] Institute of Chemistry and Technology of Materials, Graz University of Technology (NAWI Graz), Stremayrgasse 9, 8010 Graz, Austria
[b] Novocontrol Technologies GmbH & Co. KG, Aubachstr. 1, 56410 Montabaur, Germany
[c] Alistore – ERI European Research Institute, CNRS FR3104, Hub de l'Energie, Rue Baudelocque, F-80039 Amiens, France

ARTICLE INFO

Keywords:
Impedance conductivity
Stray capacitance
Electrical relaxation
Measuring methods
Solid electrolytes
Dielectric materials

ABSTRACT

The determination of the dielectric response properties is essential to the investigation of solid ion conductors. The stray capacitance contributions of the measuring cell must be systematically determined and subtracted from the acquired data. Hereby, we report and discuss a general method that can be used for the accurate determination of stray capacitance in impedance measuring cells. Our method can be applied to all commercial or custom-made impedance cells or sample holders used for variable temperature conductivity measurements of fast ion conductors. After the description of the method, we present the experimental calibration done for a 2032-type coin cell sample holder. The 2032-type coin cell is a highly reliable sample holder for impedance measurements of air sensitive materials. We tested the method on a known sample and we validated it by comparing with the results obtained in a simple reference configuration. Our simple, efficient and robust method for the determination of parasitic capacitive contributions may serve as an example of good practice in the field of solid electrolytes, solid state batteries and dielectric materials investigations.

1. Introduction

Solid-state batteries are one of the next generation energy storage technologies. By allowing the use of metal anodes, solid state batteries equipped with thin solid electrolytes present a high specific energy. [1] Nevertheless, solid-state batteries are hitherto not fully developed into a commercial technology. There are many fundamental and technological aspects still requiring proper clarifications and adequate technical solutions. [2]

Solid ion conductors used as solid electrolytes are the enabling technology for solid-state batteries. New materials, featuring high ionic conductivity [3] and preferably good chemical and electrochemical resistance against parasitic decomposition reactions are being currently pioneered and investigated. Fast ion conductors encompass a broad range of material types such as inorganic ceramic ion conductors, [4–6] polymers, [7] hybrid solid electrolytes [8–10] *etc.*

Solid electrolytes are under intense scientific and technologic scrutiny by academia and industrial actors. One key investigation, ubiquitous to solid electrolyte studies, is the measurement of ionic conductivity as a function of temperature. The conductivity is usually determined by impedance measurements, carried out by applying an alternating sinusoidal voltage while recording the resulting alternating current and its phase shift. Alternating current (AC) measurements may span a broad frequency range from GHz to μHz domain. Yet, in most cases, a frequency range between 10 MHz and 10 mHz is sufficient for the majority of conductivity investigations, although higher frequencies are desired for electrical relaxation measurements of very fast ion conductors.

At the mentioned usual frequencies, *i.e.* below 10 MHz, variable temperature conductivity data is rich in information related to electrical relaxation phenomena, including long range ion transport. Different analytical or numerical models can be used for fitting, simulating and interpreting the conductivity data. Various parameters pertaining to ion conduction and dielectric relaxation phenomena in ion conducting materials can be determined from AC conductivity data. Such parameters are the real and imaginary part of the electric permittivity and the electric modulus, the loss factor *etc.* Many parameters depend on the electric capacitance of the measured sample, which must be determined as accurately as possible. This requires beforehand the determination of stray (*i.e.* parasitic) capacitances of the measuring cell, that must be carefully accounted for and subtracted from the overall impedance response.

Very often, ion conducting materials present more than one time

* Corresponding author at: Institute for Chemistry and Technology of Materials, Graz University of Technology (NAWI Graz), Stremayrgasse 9, 8010 Graz, Austria.
E-mail address: hanzu@tugraz.at (I. Hanzu).

https://doi.org/10.1016/j.ssi.2023.116169
Received 28 December 2022; Received in revised form 3 February 2023; Accepted 6 February 2023
Available online 18 February 2023

constant at which the material relaxes in an alternating electric field, within the probed frequency range. In the simplest approximation, a parallel RC equivalent circuit is used to model a time constant. More often than not, a constant phase element (CPE) is used instead of a capacitor, as the capacitive part of the electric response deviates from the response of an ideal capacitor. In such a case, the typical equivalent circuit is represented as RQ, which is a parallel connection between a resistor and a CPE.

The value of the capacitance or the value of the CPE of the sample may be used to assign ion conduction through a specific path or part of the material. In a seminal paper, Irvine and West, have shown that in a polycrystalline solid material, the bulk and grain boundary contributions can be distinguished and assigned based on the value of the capacitance. [11] Thus, in the so-called "brick layer model", values of capacitances in the pF range are typically assigned to the bulk process, whereas capacitance values in the nF range correspond to a grain boundary process. It has to be mentioned that such values are recorded only when the thickness of the sample is in the order of 1 mm. As the vast majority of the samples are measured in the form of pressed disk pellets with a thickness in the order of 1 mm, this quick identification method of the bulk and grain boundary contributions is certainly useful. Nevertheless, for thin films with a thickness in the μm range, the capacitance deviate significantly from the values given above.

Accurate capacitance determination is thus a requirement for a valid dielectric response analysis of any ion conducting material. As many fast ion conductors are air and moisture sensitive, special experimental setups are required for impedance measurements. The special measurement cells and experimental configurations may introduce stray capacitances that must be known in order to compensate them.

2. Experimental

To determine the stray capacitance of a coin cell, five coin cells (2032-type) with different thickness of PTFE (Angst + Pfister AG) were assembled, as shown in Fig. 1 (b). For this, PTFE disks, 16 mm in diameter, were cut using a circular cutting tool (Fischer Darex circular hollow punches). By using stacked PTFE foils of two different thicknesses, *i.e.* 0.5 mm and 0.8 mm, the following coin cells were assembled (see Table 1).

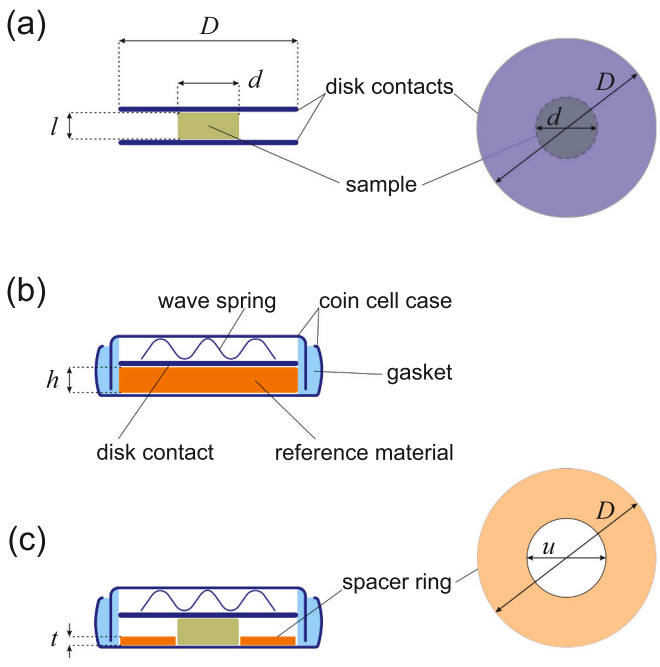

Fig. 1. a) The parallel plate configuration commonly used for dielectric relaxation (impedance) measurements. b) Cross-section diagram of a coin cell assembled with a reference dielectric material (*e.g.* PET, PTFE) for which the relative permittivity ε_r is known. This is the configuration used to acquire the calibration curve. c) Cross-section diagram of a coin cell used for the encapsulation and the impedance measurements of air sensitive samples. A thin dielectric spacer ring is used for maintaining the position of the sample pellet.

Before coin cell assembly, the PTFE foils and the 2032-type coin cell parts (PI-KEM) were dried at 333 K under vacuum in a Büchi glass oven. They were then transferred into an Argon filled glove box without any further contact with the ambient atmosphere. In the glove box, the coin cells were closed with a hydraulic crimping machine MSK-110 from MTI. 50 kg/cm^2 pressure were used to crimp the coin cells. This procedure is identical to the method used to assemble coin cells with air-sensitive pellets. The different parts of the coin cells and their dimensions are listed in Table 2.

After crimping, the coin cells were taken out of the glove-box and fitted into the ZGS active cell of a Concept 80 high performance impedance spectrometer (Novocontrol Technologies) equipped with the Alpha-A impedance analyzer and the QUATRO Cryosystem for temperature control, all instruments being operated with WinDETA v5.73 software. Calibration measurements were done at 213 K, 253 K, 293 K, 333 K and 373 K. In order to only record the capacitance of the cell, without any WinDETA software corrections, the "Cell Stray + Spacer Capacity" (C_{sccs}) parameter was set to zero while the diameter of the electrodes and the distance between electrodes were set to 0.1 mm and 10 mm respectively. This ensures that there is no capacitance correction done by the WinDETA acquisition software and that the geometrical capacitance is negligible. Thus, the parallel capacitance measured (C_p) is the actual total capacitance of the coin cell.

For the validation of the 2032-type coin cell sample holder, as shown in Fig. 1 (c), a rectangular MgO single crystal slab (6.1 × 4.1 mm^2, 1.56 mm thick) was cleaved from a larger MgO single crystal. The MgO reference crystal was immediately transferred to an Ar-filled glove-box in order to prevent any degradation of the freshly cleaved faces by the atmospheric moisture. Au contacts (50 nm thick) were applied on both crystal slab faces, in the glove-box, using a Leica sputter coater EM, ACE200. The Au-coated sample was taken out of the glove-box and the crystal rims were dry polished with 1200-grit sand paper to remove the unwanted Au layer from the rims of the slab. The dimensions of the reference crystal were determined, the reference sample was placed in the ZGS active cell and the capacitance was measured by AC impedance in the parallel disk configuration, as shown in Fig. 1 (a). After the first impedance measurement, the same reference sample was taken again into the glove-box where it was placed in a 2032-type coin cell which was crimped at a pressure of 50 kg/cm^2. No PTFE spacer ring was used. A second reference sample capacitance determination was done in the coin cell configuration, see Fig. 1 (c).

3. Results and discussion

3.1. Impedance cell configuration

The parallel plate capacitor is the most usual configuration used for conductivity measurements in solid materials, as well as for dielectric relaxation measurements in solids. In practice, the material is most commonly shaped into a disk pellet, by uniaxial pressing, a step that may optionally be followed by sintering. Once metal electrodes are applied

Table 1
PTFE foil stacking in calibration cells assembled as shown in Fig. 1 (b).

Name	PTFE foils	PTFE thickness (mm)
Calibration cell 1	1 × 0.5 mm	0.5
Calibration cell 2	1 × 0.8 mm	0.8
Calibration cell 3	2 × 0.5 mm	1
Calibration cell 4	1 × 0.5 mm + 1 × 0.8 mm	1.3
Calibration cell 5	2 × 0.8 mm	1.6

Table 2
CR-2032 coin cell parts used for coin cell assembly.

Name	Materials and Dimensions
CR-2032 negative cup	stainless steel, polypropylene gasket
CR-2032 positive cup	stainless steel
CR-2032 wave spring	stainless steel, ϕ 14.5 mm; foil thickness 0.3 mm
CR-2032 disk contact	stainless steel, ϕ 15.5 mm; thickness 0.5 mm

on the disk faces (*e.g.* Au sputtering, Ag silver paste *etc.*), the sample can be placed in the impedance measuring cell. Very rarely will the impedance measuring cell have the same dimensions as the sample pellet. Usually, the disk contacts of the impedance cell will be larger than the diameter of the pellet sample, as shown in Fig. 1 (a). Thus, there will be a non negligible stray capacitance corresponding to the gap between the contacts of the impedance measuring cell, *i.e.* in the space not occupied by the sample pellet. The capacitance calculated considering the void space occupied by the pellet is called the geometrical capacitance. The geometrical capacitance is usually calculated from the dimensions of the pellet. The capacitance C of a parallel plate capacitor is given by the expression

$$C = \varepsilon_0 \varepsilon_r \frac{A}{l} \tag{1}$$

where ε_0 is the (absolute) vacuum electrical permittivity, ε_r is the relative permittivity of the dielectric ($\varepsilon_r = 1$ in a vacuum), A is the area of the electrodes (*i.e.* the area of the metalized sample pellet face) and l is the distance between electrodes (*i.e.* the thickness of the sample pellet).

The stray capacitance can be easily calculated in the simple configuration shown in Fig. 1 (a). The stray capacitance C_s corresponds to the space between the contacts of the impedance cell which is not occupied by the sample pellet. For disk electrodes and disk pellets the stray capacitance in this simple configuration is

$$C_s = \varepsilon_0 \varepsilon_r \frac{\pi}{4} \left(\frac{D^2 - d^2}{l} \right) \tag{2}$$

where D is the diameter of the large contact disks of the impedance cell and d is the diameter of the sample pellet. Please note that Eq. 2 is valid only if $l \ll D$, otherwise edge capacitance compensation (see below) is required. [12]

In practice, the geometrical capacitance C_g and the stray capacitance C_s must be known. C_g is used, for instance, for the determination of the electrical permittivity of the sample. Indeed, the relative electrical permittivity of the sample is the ratio between the measured capacitance of the sample and the geometrical capacitance defined above. Obviously, the stray capacitance C_s must be subtracted from the acquired data in order to accurately account only for the experimental capacitance of the sample. In addition, edge compensation is required whenever the thickness l of the sample is similar to the diameter D of the impedance cell electrodes. [12]

The simple parallel plate capacitor configuration works very well for samples that are not air sensitive. For air sensitive samples the measurements must be done under protective atmosphere, either in a glove-box, or, with the sample protected in a case. Both solutions have advantages and disadvantages.

On the one hand, it can be challenging to place an impedance measuring cell inside an Ar-filled glove-box, that is commonly used for handling lithium-based battery materials, especially when variable temperature measurements are required. If the system uses a stream of nitrogen gas as a heat carrier medium, *e.g.* evaporated from a liquid nitrogen Dewar container, the piping and operation required to avoid nitrogen contamination of the glove-box are complicated. On the other hand, the possibility to use a simple stray capacitance compensation method is an advantage.

An alternative method would require an air-tight and heat-conductive sample holder in which the sample pellet can be assembled in the glove-box and then taken to the impedance measurement instrument. We found that a 2032-type coin cell is a very tight and heat conductive sample holder that can be reliably used for impedance measurements of air sensitive samples. Major advantages are a simple assembly and an almost indefinite storage duration of even the most air-sensitive samples, directly in the measuring configuration. A shortcoming is the necessity of accurately determining the stray capacitance beforehand. However, the method described below is general and it can easily be applied to determine the stray capacitance of any kind of impedance or conductivity measuring cells for solid state pellet samples.

Common 2032-type coin cells have a polypropylene gasket that may be used up to a temperature of 373 K, although special gaskets with a higher operating temperature (423 K) are commercially available, if required. For fast ion conductors, [13] which incidentally tend to have a high sensitivity to air and moisture, [14] an upper temperature limit of 373 K (100 °C) is meaningful and acceptable in many cases. A schematic of a coin cell containing a sample for impedance measurements is shown in Fig. 1 (c). For proper positioning of the sample pellet a centering ring made of a dielectric material foil, *e.g.* polyethylene terephthalate (PET, Mylar), polyamide (Nylon), polytetrafluoroethylene (PTFE) *etc.* is usually required.

3.2. Stray capacitance in coin cells

The geometry of the coin cell makes the calculation of the stray capacitance complicated, in particular in the regions near the gasket of the coin cell. However, it can easily be determined following an experimental approach. The method is based on using a reference dielectric material, with a known relative electric permittivity, that should also be as low as possible to reduce the dielectric losses. We have chosen polytetrafluoroethylene (PTFE) as it is a polymer having both a low dielectric constant ($\varepsilon_r = 2.1$) and a good thermal resistance. In addition, this reference material is commercially available in foil shape.

We start with measuring the capacitance in cells assembled with a reference material of different thicknesses, known as calibration cells, as illustrated in Fig. 1 (b). The experimentally measured capacitance C_m of a calibration cell can be expressed as

$$C_m = C_s + C_{ref} \tag{3}$$

where C_s is the stray capacitance and C_{ref} is the capacitance calculated, with Eq. 1, for a disk parallel plate capacitor of diameter D having only the reference material as the capacitor dielectric. Thus, C_{ref} corresponds only to the space between the metal plates of the capacitor filled with the reference dielectric material, all other contributions (*i.e.* stray capacitance) being excluded. Consequently, the stray capacitance of a coin cell is the difference between the measured and the reference material capacitance.

$$C_s = C_m - C_{ref} \tag{4}$$

The measured experimental capacitance C_m measured in a calibration cell, as shown in 1 (b), should vary linearly with the inverse of the thickness of the reference material $1/h$. This is true if the stray capacitance is either not influenced by the thickness of the material, or, the stray capacitance varies linearly with the thickness of the reference material. As shown in Fig. 2, we see a highly linear $C_m = f(1/h)$ plot for h values between 0.8 and 1.6 mm. In principle, the stray capacitance in a coin cell should be given by the intercept with the vertical axis of the plot of experimental capacitance *vs.* the inverse of the reference material thickness, see Fig. 2.

Indeed, when we compare the values calculated with Eq. 4 with the values obtained from the intercept of the linear plot with the vertical axis, we find very similar values. However, we also find a very small systematic error of approx 0.3–0.5 pF when we compare the vertical axis intercept value with the calculation done with Eq. 4 for a given reference

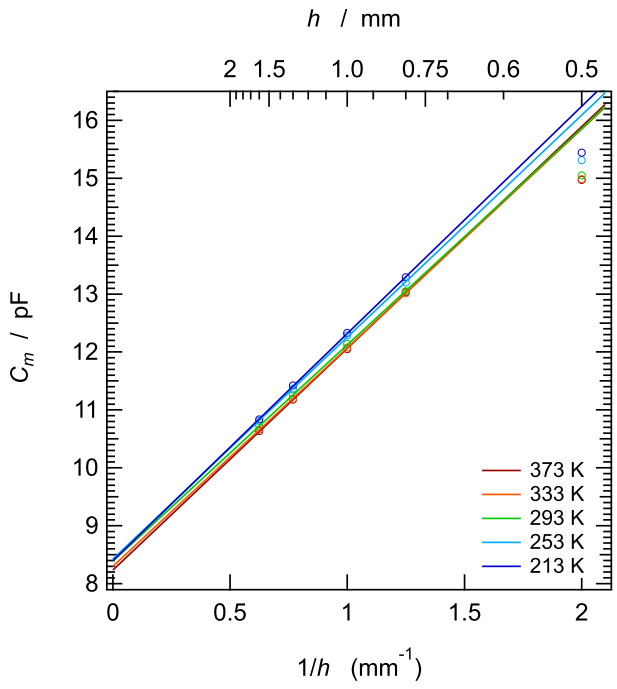

Fig. 2. Plots of the experimental capacitance measured in a coin cell in the configuration shown in Fig. 1 (b) as a function of the reciprocal thickness of the reference dielectric material $1/h$ at five different temperatures. For reference material thicknesses ranging between 0.8 and 1.6 mm the experimental capacitance varies linearly with the inverse of the reference material thickness. The solid lines are linear fits of the capacitance data *vs.* $1/h$, corresponding to reference material thicknesses ranging between 0.8 and 1.6 mm. There is a deviation from linearity for thin (*e.g.* 0.5 mm) reference material thicknesses.

material thickness. While this error is negligible for the 2032-type coin cell, it may become important in other measuring configurations or cells. Thus, it would be recommended to always evaluate the stray capacitance using the Eq. 4, rather than rely on the vertical axis intercept. For a most accurate determination of stray capacitance, this evaluation should be done at a thickness identical with the thickness of the measured sample (see below), so that the part of the stray capacitance that is dependent on the thickness of the sample, is included and correctly subtracted. This can easily be done with the Equation of the straight line resulting from the numerical data fitting (see Fig. 2) that can be used for interpolation at any given thickness of the sample. A practical implementation of this method is given in the attached CapCoin© calculation spread sheet included in the Electronic Supplementary Information section of this publication.

We also note that for thin reference materials, *e.g.* 0.5 mm in this case, there is a deviation from the linear behavior. This is however a measuring artifact, that we can trace to the limited displacement range of the wave spring used. Indeed, we found that the thin PTFE reference film are not properly flattened by the compressing wave spring and hence the lower capacity measured. Nevertheless, we note that already at 0.8 mm the linear behavior is restored. In practice, for conductivity measurements of ion conducting materials, the thickness of the pellets will be in the range 1–1.5 mm, which is fully suitable for measurements in this configuration. In accordance to experimental curves shown in Fig. 2, the coin cell configuration is ideal for pellet thicknesses ranging between 0.8 and 1.6 mm.

However, if the measurements of thin films are required, the determination of stray capacitance of the coin cell using thick reference materials is no longer valid. In such a case, the use of a slightly different measuring configuration would be required. This could be achieved by including 1–2 additional metal disk contacts or by using different wave springs offering a larger effective displacement, required to eliminate the artifact described above. Of course, a new calibration curve would have to be experimentally raised. The thickness range of reference materials used for calibration must be at least the same as the thickness range of unknown samples measured.

Last but not least, as shown in Fig. 1 (c), we note that the gap between the coin cell cups as well as the gap between the disk contacts and the coin cell cup along the horizontal direction are constant. They are dictated by the dimensions of the cell and are independent of the thickness of the sample pellet used. Thus, as these two gaps are constant we may in fact expect a value of the edge capacitance which should be mostly independent of the thickness of the pellet for 2032-type sample holders.

3.3. The overall correction capacitance

In addition to the cell stray capacitance, we have the common contributions of the impedance cell contacts, usually disk-shaped, that are usually larger than the diameter of the sample pellet, see Figure1 (a). Thus, after the determination of the stray capacitance of the cell, we have to consider the stray capacitance between the cell disk contacts, *i.e.* the capacitance of the empty space between disks. This capacitance can easily be calculated from Eq. 2, when the unoccupied space between the electrode disks is filled with a homogeneous dielectric, such as Ar or N_2.

As mentioned above, for practical reasons, a spacer ring is required for centering and holding the sample pellet in place, see Fig. 1 (c). Preferably, the spacer ring should be made of the same dielectric as the reference material. While PTFE is one of the best choices, any kind of low dielectric constant material is suitable.

In this case, the additional parasitic capacitor C_{add}, whose capacitance value has to be subtracted as well, consists of two capacitors connected in series, one having the ring material as the dielectric (C_r) and the other the gas in the coin cell as the dielectric (C_{gas}). Thus

$$\frac{1}{C_{add}} = \frac{1}{C_r} + \frac{1}{C_{gas}} \tag{5}$$

that becomes, after expressing C_r and C_{gas} from Eq. 2 with the variable notations from Fig. 1,

$$\frac{1}{C_{add}} = \frac{1}{\varepsilon_0 \varepsilon_r \frac{\pi}{4} \frac{(D^2-u^2)}{t}} + \frac{1}{\varepsilon_0 \frac{\pi}{4} \frac{(D^2-u^2)}{l-t}} \tag{6}$$

from wich the value of the additional parasitic capacitance C_{add} can be expressed

$$C_{add} = \varepsilon_0 \varepsilon_r \frac{\pi}{4} \cdot \frac{(D^2-u^2)}{t + \varepsilon_r (l-t)} \tag{7}$$

The above expression is used to calculate the parasitic capacitance of the space between the electrode disks that is not occupied by the sample, but in which a thinner spacer ring made of a reference (dielectric) material is present.

Finally, we shall note that there is a small gap between the spacer ring and the sample pellet since for practical reasons the inner diameter u of the spacer ring has to be slightly larger than the diameter d of the sample pellet. The capacitance of this gap (C_{gap}) can also be expressed, in a similar manner to Eq. 2, as

$$C_{gap} = \varepsilon_0 \frac{\pi}{4} \left(\frac{u^2 - d^2}{l} \right) \tag{8}$$

In practice we have found that for a pellet diameter of 5 mm and a spacer ring inner diameter of 6 mm, the capacitance C_{gap} is smaller than 0.1 pF and thus truly negligible, see CapCoin© calculation spread sheet from the Electronic Supporting Information section. Finally, the capacitance that must be subtracted from the impedance data acquired on a pellet sample enclosed in a coin cell as shown in Fig. 1 (c) is given by:

$$C_{corr} = C_m - C_{ref} + C_{add} + C_{gap} \quad (9)$$

The C_{corr} capacitance corresponds to the value that must be subtracted from the acquired impedance data; it can be thus input in the field "Cell Stray + Spacer Capacity" in the WinDETA software. The dimensions of the sample pellet can be introduced as usual in the impedance acquisition software (*e.g.* WinDeta), where they will be used for the calculation of the geometrical capacitance and the calculation of conductivity from the impedance data that was corrected for stray and parasitic capacitances.

Please note that C_m is an experimentally determined quantity that includes the stray capacitance contributions of the cell and of the whole experimental set-up. This quantity can easily be determined from an experimental calibration curve as shown in Fig. 2 and in the calculation spread sheet example CapCoin© (see ESI).

3.4. Comparison and validation of the method

In order to validate the experimental method, we conducted a control experiment in which we measured a single crystal MgO sample. This sample has a moderate-low air (moisture) sensitivity and therefore is suitable as a reference sample in various measuring configurations. The same sample was first measured in the parallel disk capacitor configuration, as shown in Fig. 1 (a), and then in the 2032-type coin cell configuration, as shown in Fig. 1 (c), albeit without the spacer ring, whose absence was required for the evaluation of the dielectric losses in the polypropylene gasket (see below). The comparison between the two measurements is shown in Fig. 3. We shall note that the usual experimental error corresponding to capacitance determination is in the order of 0.1 pF or below. Thus, the small difference between the two measurements, amounting to a maximum of 0.04 pF, is well within the expected error margin.

The calculated stray capacitance in the parallel disk configuration was 0.67 pF, while the determined stray capacitance in coin cell configuration was 9.45 pF. As no spacer ring was used, the stray capacitance in the coin cell configuration was determined by setting to zero the thickness of the spacer ring (t = 0 mm) in the CapCoin© calculation spread sheet. The very small increase of capacitance seen in the coin cell configuration at low frequencies can be traced to the dielectric losses in the polypropylene gasket of the coin cell, which are higher than for the MgO sample. Nevertheless, due to their very low magnitude, the dielectric loses in the polypropylene gasket can be neglected in most cases. This result and the comparison shown in Fig. 3 demonstrate the feasibility and high accuracy of impedance measurements in 2032-type coin cell configuration, as required for air-sensitive samples.

4. Conclusions

Coin cells can be used as simple, effective and very long life sample holders for electrical relaxation investigations of air sensitive solid materials. However, the geometry of the coin cells complicates the determination of the stray capacitance - the gasket and the odd shape of the coin cell makes a simple calculation complicated. We have described in detail a simple, robust and effective method for the determination of stray capacitance in coin cells and the accurate calculation of all other parasitic capacitive contributions. The experimental determination of capacitance in calibration cells makes the method robust against unaccounted systematic errors. All stray capacitance contributions are captured and included in the calibration curve. As the size and geometry of the coin cell holder is identical for different cells, the coin cell external parasitic contributions (*e.g.* due to fitting the coin cell in a temperature controlled impedance measuring chamber) are also included in the experimental calibration curve.

The method we describe here has a high degree of generality. It can be applied to the determination of stray capacitance of any kind of impedance measuring cell. Our method is thus an example of good practice to follow when measuring the AC impedance response of ion conducting materials.

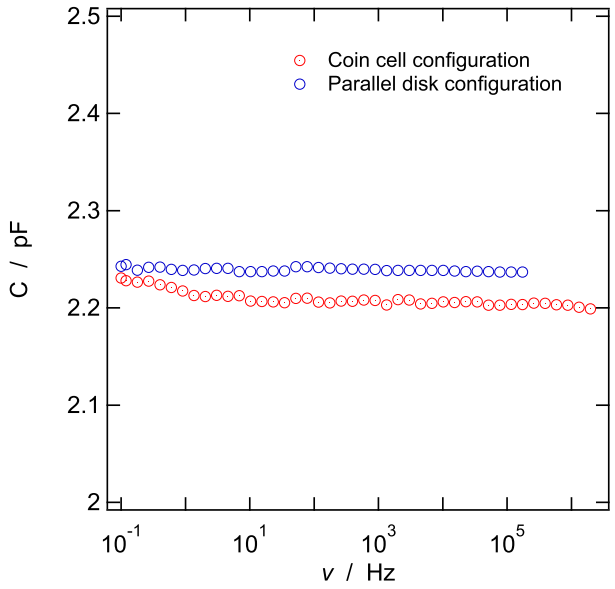

Fig. 3. Comparison between the capacitance of a single crystal MgO sample at 293 K determined first in the parallel disk configuration and then in the 2032-type coin cell configuration. The plotted values are obtained by subtracting the stray capacitances from the raw data. The raw data capacitances were in the order of 2.9 pF for the parallel disk configuration and 11.6 pF for the coin cell configuration. Yet, once the stray capacitances are subtracted, the difference between the two measurements is well below 0.1 pF, which is the range of the experimental determination error. This validates the coin cell configuration as a reliable impedance measuring cell.

CRediT authorship contribution statement

Alexander Komar: Investigation, Data curation, Validation, Visualization, Writing – original draft. **Dirk Wilmer:** Methodology, Validation, Writing – review & editing. **H. Martin R. Wilkening:** Resources, Writing – review & editing. **Ilie Hanzu:** Conceptualization, Methodology, Writing – original draft, Writing – review & editing, Supervision, Project administration, Funding acquisition.

Declaration of Competing Interest

The authors declare the following financial interests/personal relationships which may be considered as potential competing interests:

Co-author is an editor of Solid State Ionics - H.M.R.W.

Data availability

Data will be made available on request.

Acknowledgements

We thank Klaus Reichmann for useful discussions and advice on choosing a suitable reference sample. This research received funding from Land Steiermark through Zukunftsfonds Steiermark (project Hybrid-Solarzellenbatterie, grant no. 1341) and from the FFG (project SolaBat, grant no. 853627). The Deutsche Forschungsgemeinschaft (DFG) (FOR 1227 MoLiFe, project LIDINAM, grant HA6966/1-2) is also acknowledged.

Appendix A. Supplementary data

Supplementary data to this article can be found online at https://doi.org/10.1016/j.ssi.2023.116169.

References

[1] S. Randau, D.A. Weber, O. Kötz, R. Koerver, P. Braun, A. Weber, et al., Benchmarking the performance of all-solid-state lithium batteries, Nat. Energy 5 (3) (2020) 259–270, https://doi.org/10.1038/s41560-020-0565-1.

[2] T. Krauskopf, F.H. Richter, W.G. Zeier, J. Janek, Physicochemical concepts of the lithium metal anode in solid-state batteries, Chem. Rev. 120 (15) (2020) 7745–7794, https://doi.org/10.1021/acs.chemrev.0c00431.

[3] R. Zettl, S. Lunghammer, B. Gadermaier, A. Boulaoued, P. Johansson, H.M. R. Wilkening, et al., High Li^+ and Na^+ conductivity in new hybrid solid electrolytes based on the porous MIL-121 metal organic framework, Adv. Energy Mater. 11 (16) (2021) 2003542, https://doi.org/10.1002/aenm.202003542.

[4] Z. Zhang, Y. Shao, B. Lotsch, Y.S. Hu, H. Li, J. Janek, et al., New horizons for inorganic solid state ion conductors, Energy Environ. Sci. 11 (8) (2018) 1945–1976, https://doi.org/10.1039/C8EE01053F.

[5] P. Knauth, Inorganic solid Li ion conductors: An overview, Solid State Ionics 180 (14) (2009) 911–916, https://doi.org/10.1016/j.ssi.2009.03.022.

[6] D. Prutsch, S. Breuer, M. Uitz, P. Bottke, J. Langer, S. Lunghammer, et al., Nanostructured ceramics: ionic transport and electrochemical activity, Z. Phys. Chem. 231 (7–8) (2017) 1361–1405, https://doi.org/10.1515/zpch-2016-0924.

[7] K. Jeong, S. Park, S.Y. Lee, Revisiting polymeric single lithium-ion conductors as an organic route for all-solid-state lithium ion and metal batteries, J. Mater. Chem. A 7 (5) (2019) 1917–1935, https://doi.org/10.1039/C8TA09056D.

[8] X. Yu, A. Manthiram, A review of composite polymer-ceramic electrolytes for lithium batteries, Energy Storage Mater. 34 (2021) 282–300, https://doi.org/10.1016/j.ensm.2020.10.006.

[9] A. Ferbezar, R. Zettl, H. Fitzek, B. Gadermaier, I. Hanzu, Ion conduction in Na^+ containing ionogels based on the UiO-66 metal organic framework, Electrochim. Acta 434 (2022), 141212, https://doi.org/10.1016/j.electacta.2022.141212.

[10] R. Zettl, I. Hanzu, The origins of ion conductivity in MOF-ionic liquids hybrid solid electrolytes, Front. Energy Res. 9 (2021), 714698, https://doi.org/10.3389/fenrg.2021.714698.

[11] J.T.S. Irvine, D.C. Sinclair, A.R. West, Electroceramics: characterization by impedance spectroscopy, Adv. Mater. 2 (3) (1990) 132–138, https://doi.org/10.1002/adma.19900020304.

[12] G. Schaumburg, D. Wilmer, Improving the accuracy of dielectric measurements, personal communication, 2018. URL: https://www.novocontrol.de/pdf_s/Accuracy_of_Measurements.pdf.

[13] M. Gombotz, K. Hogrefe, R. Zettl, B. Gadermaier, H.M.R. Wilkening, Fuzzy logic: about the origins of fast ion dynamics in crystalline solids, Philos. Trans. R. Soc. A Math. Phys. Eng. Sci. 379 (2211) (2021) 20200434, https://doi.org/10.1098/rsta.2020.0434.

[14] A.K. Hatz, R. Calaminus, J. Feijoo, F. Treber, J. Blahusch, T. Lenz, et al., Chemical stability and ionic conductivity of LGPS-type solid electrolyte tetra-Li_7SiPS_8 after solvent treatment, ACS Appl. Energy Mater. 4 (9) (2021) 9932–9943, https://doi.org/10.1021/acsaem.1c01917.